

Computational Analysis of Pulse Detonation Engine: Effects of Converging and Diverging Tube Geometries

a project presented to
The Faculty of the Department of Aerospace Engineering
San José State University

in partial fulfillment of the requirements for the degree
Master of Science in Aerospace Engineering

by

Bhagyashree Nagarkar

December 2018

approved by

Dr. Periklis E. Papadopoulos
Faculty Advisor



© 2018

Bhagyashree Nagarkar

ALL RIGHTS RESERVED

The Designated Project Advisor Approves the Thesis Titled

COMPUTATIONAL ANALYSIS OF PULSE DETONATION ENGINE: EFFECTS OF CONVERGING
AND DIVERGING TUBE GEOMETRIES

By

Bhagyashree Nagarkar

APPROVED FOR THE DEPARTMENT OF AEROSPACE ENGINEERING

SAN JOSÉ STATE UNIVERSITY

December 2018

Dr. Periklis E. Papadopoulos

Department of Aerospace Engineering

ABSTRACT

COMPUTATIONAL ANALYSIS OF PULSE DETONATION ENGINE: EFFECTS OF CONVERGING AND DIVERGING TUBE GEOMETRIES

by Bhagyashree Nagarkar

The pulse detonation engines (PDE) are an extension of pulse-jet engines, where PDEs detonate their fuels, rather than deflagrate. In view of its advantages of high thermodynamic efficiency, light weight, low cost, variability of thrust, etc., PDEs will serve as next generation's flight technology. Initially this paper summarizes the detonation physics and development of PDEs over the years by providing computational simulations and experimental work undertaken by various research facilities. Then, a validation case for a constant area detonation is run using the CFD code provided by ANSYS Fluent. The detonation wave propagation is greatly affected by the tube geometry and hence another case validation is run by introducing an inclination along the length of the tube. Thus, converging or diverging section of the tube, increased or decreased the average wave velocity. The other detonation characteristics, especially the pressure showed variations depending upon the tube geometry.

ACKNOWLEDGEMENTS

I would like to thank Prof. Dr. Nikos Mourtos and Prof. Dr. Periklis Papadopoulos for their support, guidance and education provided for the completion of this project and throughout my graduate career. I would like to also thank my Lab partner, Samuel Zuniga, without whom the success of this project was not possible. Lastly, I would like to thank my family and my friends who stood by me through all good and bad times.

Table of Contents

List of Figures	8
List of Tables	10
Nomenclature	11
CHAPTER 1 INTRODUCTION	12
1.1 Background and Motivation.....	12
1.2 Detonation Physics.....	14
1.2.1 Deflagration versus Detonation	14
1.2.2 Steady State versus Unsteady State Engines.....	14
1.2.3 CJ Theory.....	15
1.2.4 ZND Detonation Wave Structure.....	18
1.2.5 ZND Detonation Wave Propagation	21
1.3 Concept of Pulse Detonation Engine	22
1.3.1 Pure PDE Cycle	22
1.3.2 PDE Concept Model	23
1.3.3 Advantage of PDE	23
1.3.4 Flight Applications of PDE.....	24
1.4 Literature Review.....	26
1.4.1 Reviews on Experimental Studies.....	26
1.4.2 Reviews on Computational Modeling Studies	30
1.5 Project Proposal	35
1.6 Methodology	35
CHAPTER 2 COMPUTATIONAL ANALYSIS SETUP	37
2.1 Detonation Initiation	37
2.1.1 Direct Initiation.....	37
2.1.2 Deflagration to Detonation Transition (DDT).....	37
2.3 Chemical Kinetics	38
2.4 Converging and Diverging Detonation Tube Geometries.....	40
2.5 Boundary Conditions Setup	41
2.6 CFD Solver	41
CHAPTER 3 GOVERNING EQUATIONS	44
CHAPTER 4 CASE VALIDATION: EFFECTS OF TUBE GEOMETRY	47
4.1 Case 1: 1-D Wave Propagation in a Constant Area Tube	47

4.2 Case 2: 1-D Wave Propagation in Varying Area Tube	49
CHAPTER 5 RESULTS AND DISCUSSION	51
5.1 Constant Area Rectangular Tube	51
5.2 Simulation vs. NASA CEA.....	54
5.3 Varying Area Tube.....	55
Bibliography	63
APPENDIX.....	66
Appendix A.....	66
Appendix B	Error! Bookmark not defined.
Appendix C	69

List of Figures

Figure 1 Russia State Corporation for Space Activities (RosCosmos) Prototype of PDE (Vizcaino, 2013)	12
Figure 2 Detonation wave in constant area tube	16
Figure 3 Rayleigh line - Hugoniot curve PV diagram	16
Figure 4 Variation of physical properties for ZND conditions	19
Figure 5 Location of von Neumann spike	20
Figure 6 "Fish scale" structure of the detonation wave (Valli & Jindal, April 2014)	20
Figure 7 ZND Pressure Profile within the detonation tube	21
Figure 8 Pure PDE operating cycle	22
Figure 9 Structure of PDE concept model	23
Figure 10 PDE- hybrid gas turbine engine (a) detonation wave propagation in tube, (b) placement of detonation tubes	25
Figure 11 General PDE experimental setup with Shchelkin spiral	28
Figure 12 Multi-cycle simulations showing temperature contours	31
Figure 13 Schematic of supersonic air-breathing PDE	32
Figure 14 Computational PDE model with dimensions (including choked inlet, intake tube, and constant fuel mass flow)	33
Figure 15 Schematic of a Valve-less PDE setup	33
Figure 16 Supersonic Flow in Converging -Diverging Section	41
Figure 17 Algorithm for Density Based solver in ANSYS Fluent	42
Figure 18 Schematic of 2-D Axisymmetric Ideal PDE tube	47
Figure 19 2-D Adaptive mesh of ideal PDE tube	47
Figure 20 Initial conditions for the ideal PDE tube with pressure contour	49

Figure 21 PDE tube with positive angle of inclination (α).....	49
Figure 22 PDE tube with negative angle of inclination (α)	50
Figure 23 Initial conditions for PDE tube having positive inclination with pressure contour.....	50
Figure 24 Initial conditions for PDE tube having negative inclination with pressure contour.....	50
Figure 25 Detonation wave propagation along the ideal PDE tube with Pressure contours.....	51
Figure 26 ZND Pressure profile	52
Figure 27 ZND Temperature profile	53
Figure 28 Detonation wave propagation along the PDE tube with positive inclination showing pressure contours	56
Figure 29 Detonation wave propagation along the PDE tube with negative inclination showing pressure contours	56

List of Tables

Table 1 Setup and initialization conditions unburned gas mixture	48
Table 2 Setup and initialization conditions for ignition region	48
Table 3 Wave velocity measurement.....	54
Table 4 CJ conditions.....	55
Table 5 Variations of Pressure in PDE tube with inclinations	57
Table 6 Wave velocity measurement for $\alpha = -3^\circ$	58
Table 7 Wave velocity measurement for $\alpha = -2^\circ$	59
Table 8 Wave velocity measurement for $\alpha = -1^\circ$	59
Table 9 Wave velocity measurement for $\alpha = +1^\circ$	60
Table 10 Wave velocity measurement for $\alpha = +2^\circ$	60
Table 11 Wave velocity measurement for $\alpha = +3^\circ$	61

Nomenclature

$1-D$	One Dimensional
PDE	Pulse Detonation Engine
CJ	Chapman Jouget
ZND	Zeldovich-von Neumann-Doring
CD	Convergence Divergence nozzle
P_1, P_2	Pressure upstream and downstream
ρ_1, ρ_2	Density upstream and downstream
v_1, v_2	One – dimensional velocity
h_1, h_2	Enthalpy of the fuel/oxidizer (per unit mass)
q	Heat addition (per unit mass)
Eq.	Equation(s)
ϑ_1, ϑ_2	Specific volume
μ	Wave speed
e	Internal energy of fuel/oxidizer

CHAPTER 1 INTRODUCTION

1.1 Background and Motivation

The pulse detonation engine (PDE) is an unsteady propulsion system that utilizes the high rate of energy release from detonation waves to produce thrust (Yungster, 2003). A simple physics of detonation-based combustion is used to achieve higher performance than current, steady state deflagration-based engines. This detonation-generated thrust reduces the need for high pressure pumps or engine compressor, and in doing so, give a significant advantage over current air-breathing propulsion systems.

An ideal PDE consists of a constant area tube closed at one end, and open to the atmosphere at the other end. PDE generates thrust at irregular intervals, which produces a significant pressure rise in combustor region by adding heat at constant volume. (Ma, 2003) Thus, PDE cyclically detonates fuel and atmospheric air mixtures to generate thrust.



Figure 1 Russia State Corporation for Space Activities (RosCosmos) Prototype of PDE

(Vizcaino, 2013)

Using detonation in PDEs results in large pressure and temperature increases, as the combustion region is coupled to a supersonic shock wave. (Glassman & Yetter, 2008) Thus

detonation is a much more energetic and violent phenomena than deflagration. For modeling and understanding of PDEs, the complex nature of the detonation waves is simplified with the use of Chapman-Jouguet (C-J) and Zeldovich-von Neumann-Doring (ZND) models, which will be discussed in brief in the following section.

PDEs became the first practical, experimentally-tested detonation engines in the 1990s. (Ma, 2003) While they are simple and efficient in many ways, PDEs have many engineering challenges yet to be resolved. One of the main challenges is the requirement for repeated initiation of detonations within the detonation chamber. Another major challenge, is the timing and control of valving the fresh reactants for efficient performance. This complex system adds weight to the propulsion system. (Srihari & Mallesh, 2015) Other challenges include the length of the tube required to achieve deflagration to detonation transition (DDT) which increases the combustor size; and the limited operating frequency attained so far.

In recent years, numerous studies and experiments have been done regarding the development of detonation initiation, nozzles and ejectors, and system level performance estimates in order to overcome the above-mentioned challenges. (Ebrahimi, 2002) The key features of PDEs are rapid combustion species and energy conversion, to attain a specific detonation velocity and desired thrust. Some of the initial research work done by Eidelman and Grossmann (Eidelman, “Review of Propulsion Applications and Numerical Simulations of The Pulse Detonation Engine Concept, 1991) have been reviewed in the following section, to understand the work done in the late 1980s on PDEs. The basic PDEs theory and concept studied by Bussing and Pappas (T. & G., 1995) have been discussed. The focus of this chapter is more on the review of performance estimates from various experimental, numerical, and computational studies.

1.2 Detonation Physics

1.2.1 Deflagration versus Detonation

The process of combustion is related to energy release by deflagration or detonation.

Deflagration is the most common type of combustion and is considered as isobaric, or a constant pressure process. (T. & G., 1995) Here the combustion propagates via heat transfer; hot burning fuel-oxidizer mixture heats the next layer of unburnt mixture and ignites it. The speed at which fuel-oxidizer mixture burns is subsonic and is a controllable process. Deflagration burns outward radially, and the speed of propagation depends upon the availability of fuel. For example, the combustion process in gas turbine engines.

Detonation is a supersonic combustion process, where the decomposition/ combustion reaction releases a lot of energy in short span of time, resulting in large overpressures (up to 20 bars) and high propagating velocities (up to 2000 m/s). (Yungster, 2003) Thus, detonation is a constant volume combustion process with a supersonic shock wave.

1.2.2 Steady State versus Unsteady State Engines

Based on the combustion process employed, the air-breathing engines are grouped as steady (quasi-steady) or unsteady. (T. & G., 1995) The steady state engines are characterized by deflagration-based combustion process and are the most widely used class of engines. Examples of this type are turbojets and ramjet engines.

Unsteady engines can be either deflagration-based or detonation-based combustion. (Srihari & Mallesh, 2015) In this class of devices, the combustion is based on burned fuel/oxidizer speeds, and combustion chamber characteristics. For example, pulse jet engines and PDEs.

1.2.3 CJ Theory

For studying PDE performance, the detonation waves can be modeled as discontinuities in the flow of an ideal fuel-oxidizer at which heat addition occurs (Ma, 2003). This modeling describes basic detonation wave physics of a 1-D propagation in a constant area tube.

As per conservation equations for mass, momentum, and energy for detonation waves and equation of state (Thattai, 2010) (5 A combustion wave in a premixed gas, the Chapman-Jouguet detonation wave, n.d.);

Mass continuity:

$$\rho_1 u_D = \rho_2 (u_D - u_2) \quad (2.1)$$

Momentum conservation:

$$p_1 + \rho_1 u_D^2 = p_2 + \rho_2 (u_D - u_2)^2 \quad (2.2)$$

Energy equation:

$$\frac{\gamma p_1}{\gamma - 1} + \frac{1}{2} \rho_1 u_D^2 + q = \gamma \frac{p_2}{\gamma - 1} + \frac{1}{2} \rho_2 (u_D - u_2)^2 \quad (2.3)$$

where the velocities relative to wave front are expressed as those relative to the tube; u_D being the detonation velocity, γ is the specific heat ratio, subscript 1 denotes the unburned gas or reactants, state and subscript 2 for the final state of burned gas behind the detonation wave (Figure 2) (Ma, 2003).

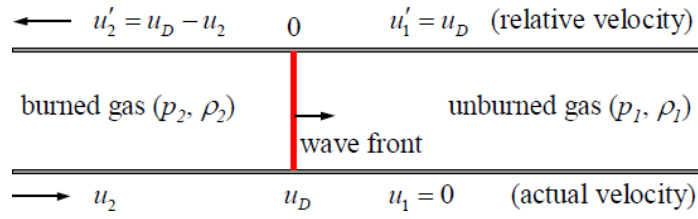


Figure 2 Detonation wave in constant area tube

Combining Eq. (2.1) and (2.2) to get Rayleigh relation,

$$\frac{(p_2 - p_1)}{\frac{1}{\rho_2} - \frac{1}{\rho_1}} = -\rho^2 u^2 \quad (2.4)$$

Rearranging Eq. (2.1) to (2.3) results in the following relation referred to as Hugoniot relation,

$$\frac{\gamma}{\gamma - 1} \left(\frac{p_2}{\rho_2} - \frac{p_1}{\rho_1} \right) - \frac{1}{2} (p_2 - p_1) \left(\frac{1}{\rho_2} + \frac{1}{\rho_1} \right) = q \quad (2.5)$$

The Hugoniot expressions relate the thermodynamic properties upstream and downstream of a combustion region. These two relations given by Eq. (2.4) and (2.5) is plotted as p_2 verses $1/\rho_2$ plane to get a Rayleigh line and Hugoniot curve as in Figure 3 (Ma, 2003).

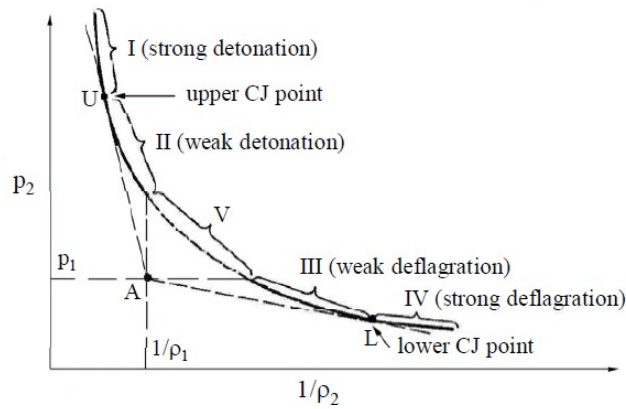


Figure 3 Rayleigh line - Hugoniot curve PV diagram

In the above figure, the point A denotes the unburned gas state through which all Rayleigh lines pass. Among these lines there are two which are tangent to the Hugoniot curve and the corresponding tangent points are the CJ points where points, U and L refer to the upper and lower CJ points respectively. The upper CJ point represents minimum detonation velocity while the lower corresponds to a minimum detonation velocity. The horizontal and vertical Rayleigh lines passing through point A relates to constant-pressure and constant-volume processes. Thus, the possible state outcome depends on the intersection of Rayleigh line and Hugoniot curves.

The CJ condition is given as;

$$v = u_D - u_2 = \frac{\sqrt{p_2}}{\rho_2} = a'_2 \text{ or}$$

$$M'_2 = \frac{v_2}{a'_2} = 1 \quad (2.6)$$

Based on the relation of the velocity of burned gas relative to the wave front, the Hugoniot curve is divided into five regions, from regions I to V as in figure where regions I and II are detonation section having a supersonic wave front velocity; regions III and IV denoting the deflagration section with a subsonic wave front velocity (Ma, 2003) (Lam, Tillie, T., & B., 2004).

In region I the supersonic flow is converted to subsonic; i.e., $u_2 + a_2' > u_D$. Hence, this region is referred to as strong detonation or overdriven detonation region, and is unstable. There are chances that any rarefaction waves arising behind the wave front will overtake and weaken the detonation wave, by reducing the pressure while decreasing the final values of P_2 and $1/\rho_2$. The rarefaction waves can form due to heat losses, turbulence, or friction. Thus, the solutions in this region are possible only for transient state.

Region II is known as weak detonation region with flow remaining supersonic; i.e., $u_2 + a_2' < u_D$. Here, the structure of the detonation wave is a shock wave followed by chemical reaction leading to heat addition. But for a steady flow in constant-area tube, the fluid cannot be accelerated to from subsonic to supersonic, therefore no solution exists in region II. Similar conditions are observed in Region IV which is known as a strong-deflagration region. The density decreases, and due to heat addition the wave is accelerated from subsonic to supersonic. Thus, region IV is physically impossible and a strong-deflagration is never observed.

Region III is known as the weak-deflagration region as the deflagration wave propagates at subsonic velocity. The pressure is reduced and the flow remains subsonic.

Thus, at the point U, the velocity of the detonation wave is equal to the velocity of sound in the burned gases; $u_D = a_2'$, as well as the mass velocity of those gases, and no rarefaction will overtake it. This makes point U a “self-sustained” detonation and is referred to as the C-J result.

The detonation velocity in CJ condition is calculated with no knowledge of the chemical reaction rate or structure of the wave.

1.2.4 ZND Detonation Wave Structure

In the early 1940s, Zeldovich, von Neumann, and Doring independently arrived at a theory for the structure of the detonation wave where the kinetics and mechanism of the reaction give the time and spatial separation of the front and the C-J plane (Figure 4). Their theory states that a detonation wave is a planar shock wave propagating at detonation velocity while leaving heated and compressed burned gas behind it. This shock wave while propagating, also provides activation energy to ignite unburned gases, whereas the energy released by the reaction keeps the shock moving. (Glassman & Yetter, 2008) ZND wave theory also assumes that no reaction takes place

in the shock wave region due to its width being in the order of few mean free paths of the gas molecules, whereas the width of the reaction region is in order of one centimeter (Ma, 2003) (Lam, Tillie, T., & B., 2004).

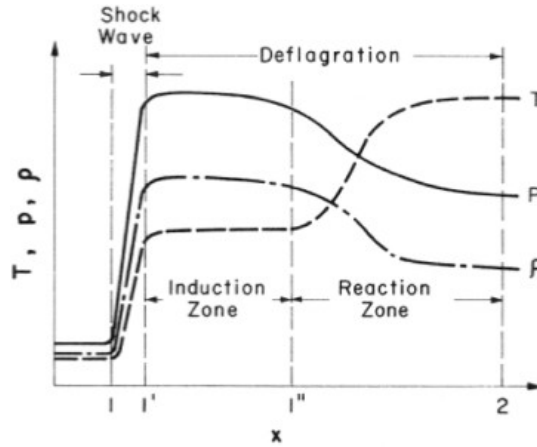


Figure 4 Variation of physical properties for ZND conditions

The above diagram shows a graphical variation of density, pressure and temperature of a detonation wave travelling to the left through unburned gases. Plane 1 denotes the state of unburned gas just before the occurrence of shock wave. Plane 1' denotes the state when detonation occurs and state immediately behind the shock wave. The deflagration region begins from plane 1' and finishes at plane 2, where the system reaches CJ state. This region is divided into induction zone and reaction zone, based on the kinetics of the gas mixture. Due to the slow rate of the chemical reaction the density, pressure and temperature are relatively flat, and temperature is not very high. While in the reaction zone heat addition takes place due to increase in rate of reaction, thus drastically changing the gas properties.

The stage right after the shock wave high pressure is generated due to shock wave compressing the gas. This is denoted as the intersection point of the shock Hugoniot curve and the

Rayleigh line above the upper CJ section. This point is referred to as the von Neumann spike (Figure 5). This phenomenon occurs at zero chemical reaction rate.

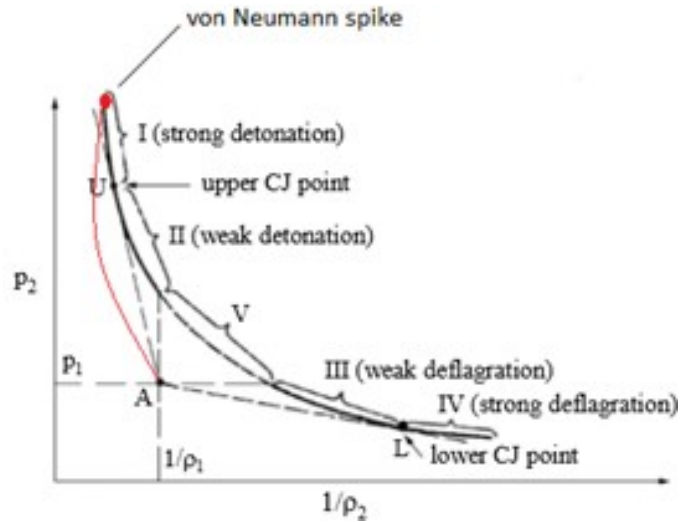


Figure 5 Location of von Neumann spike

The complex cellular three-dimensional structure of the detonation wave is experimentally observed and is generally referred as “fish-scale” structure (Figure 6). The characteristic size of the fish scale like structure refers to the detonation cell size (λ).

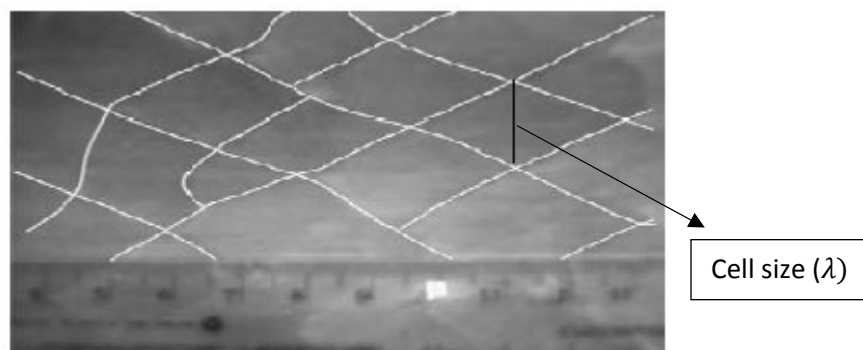


Figure 6 "Fish scale" structure of the detonation wave (Valli & Jindal, April 2014)

1.2.5 ZND Detonation Wave Propagation

The detonation wave propagates in a constant –area tube closed at one end. This is followed by a rarefaction wave and a uniform region, shows pressure profile within the tube. (Ma, 2003)

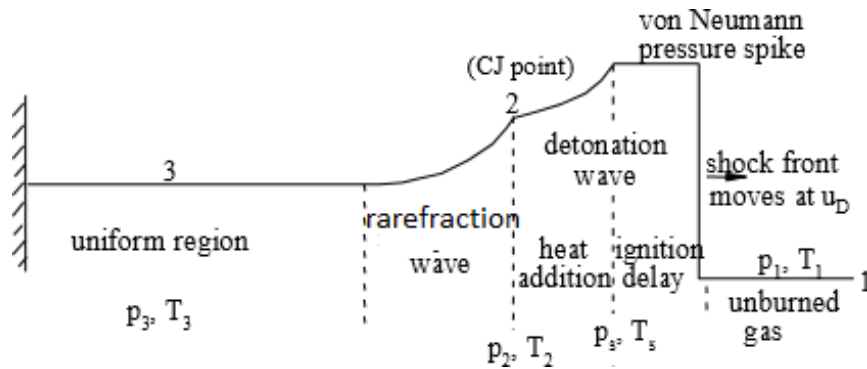


Figure 7 ZND Pressure Profile within the detonation tube

For a ZND model following quantitative properties are observed. This table also provides the difference between detonation and deflagration parameters. (Vizcaino, 2013)

Table 2 Detonation vs. Deflagration Quantitative differences

Ratio	Usual magnitude of Ratio	
	Detonation	Deflagration
U_u/C_u^a	5-10	0.0001-0.03
U_b/u_u	0.4-0.7	4-16
P_b/P_u	13-55	0.98-0.976
T_b/T_u	8-21	4-16
ρ_b/ρ_u	1.4-2.6	0.06-0.25

^a C_u is the acoustic velocity in the unburned gasses. U_u/C_u is the Mach number of the wave.

1.3 Concept of Pulse Detonation Engine

Detonation engines consist of three categories: Oblique Detonation Wave Engine (ODWE) where the burned fuel/oxidizer mixture velocity equals or exceeds C-J velocity, Continuous or Rotational Detonation Engine (CDE / RDE) where burned fuel/oxidizer mixture is injected along axial direction with the detonation wave propagating in azimuthal direction, and lastly PDEs which operate on pure PDE cycle.

1.3.1 Pure PDE Cycle

The pure PDE cycle begins by filling the detonation combustion chamber with a detonable mixture. Detonation is initiated with an initiation device at the closed end of the tube. (Yungster, 2003) (Ma, 2003) A detonation wave compresses the fuel/oxidizer as it travels through the combustor which results in rapid release of heat and a sudden rise in pressure. It is during this interval of time, that most of the PDE thrust is produced. The detonation wave exits at the open end of the tube into surrounding air followed by the burned gases, also known as purging stage. When the conditions within the tube reach a specified state, the tube is supplied with a fresh detonable mixture (filling stage), and the cycle is repeated as in Figure 8. This pure PDE cycle is repeated 20-100 times per second to produce thrust.

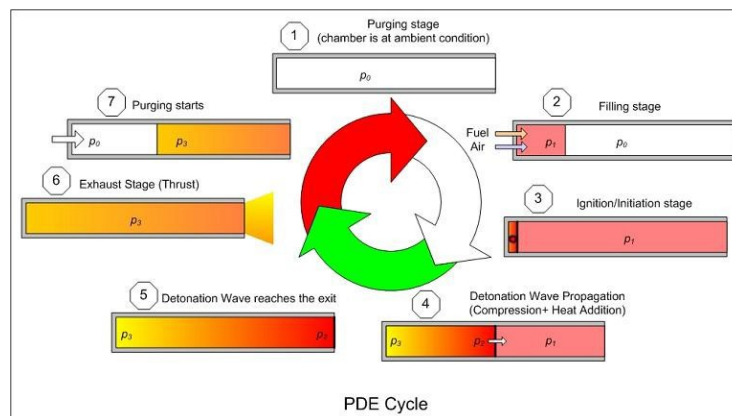


Figure 8 Pure PDE operating cycle

1.3.2 PDE Concept Model

A detonation is created via DDT or direct detonation. DDT begins with a deflagration initiated using a weak energy source, then increasing the pressure and temperature leads to formation of detonation wave. However, this process can take over a several meters of tube length and large amount of time. Direct initiation is dependent upon an ignition source driving a detonation wave of sufficient thrust which travels down the detonation tube, and exit in the atmosphere through a nozzle.

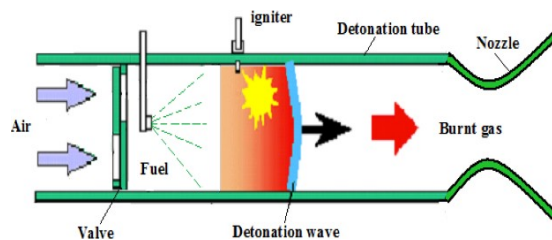


Figure 9 Structure of PDE concept model

For efficient functionality of PDEs, it is needed to minimize the cycle time and maximize thrust, also the ignition and mixing must occur quickly. It is necessary to shorten DDT distances as this further decreases the PDE cycle, allowing frequency and thrust increase. An air-breathing PDE model typically consists of an air inlet with fuel injector located at the inlet or head end of detonation tube. DDT augmentation ignitor device is placed in the detonation section of the combustor. Finally, a nozzle is attached at the open end of the tube to enhance the engine thrust by a blowdown process. (Srihari & Mallesh, 2015)

1.3.3 Advantage of PDE

The rate of release of chemical energy during a combustion process defines the propulsive efficiency of a vehicle. For a detonation based combustion this energy is three times of magnitude

higher than in a deflagration based combustion process. (Helman, June 1986) A pulsed mode of operation is utilized in PDEs to control the rate of combustible mixture supply. This eliminates the need for any heavy built fuel injection pump machinery, which further helps in decreasing the weight of the propulsion system. Additionally, the high pressure generated by detonation wave compresses the gas, thus further mitigating the need for compressors or turbines which are used in current air-breathing engines. Thus, the lower machinery part count contributes to easy maintenance of PDEs. This also contributes to an overall weight decrease, improving thrust-to-mass ratio and lowering the cost of the PDE system (Yungster, 2003).

The constant volume combustion cycle in a PDE gives the advantage of thermodynamic efficiency and reduced CO emissions as compared to constant pressure combustion cycle in deflagration based engines. The thermodynamic cycle efficiency of a PDE is 30% to 50% higher than other cycle efficiencies for a chemically reacting hydrogen-air (fuel-oxidizer) mixture (Bussan) thus resulting in higher specific impulses. A good operating frequency results in good performance and based on this, efforts are being made over several decades to improve and establish a controlled detonation (Lam, Tillie, T., & B., 2004).

1.3.4 Flight Applications of PDE

As Pulse Detonation Engines have numerous potential advantages over current air-breathing and other space propulsion systems, PDEs find many applications in the aerospace industry. One of the interesting proposed application of PDE propulsion includes the combination of a PDE and turbine cycles. (Lam, Tillie, T., & B., 2004) PDE-hybrid gas turbine engines, where the continuous flow combustor is replaced with multiple pulsed detonation chambers (Figure 10). These engines can then be used for a faster, more efficient and environmental friendly commercial

and military aircraft. But the operating cycle combination of PDE and gas turbine is a matter of considerable complexity.

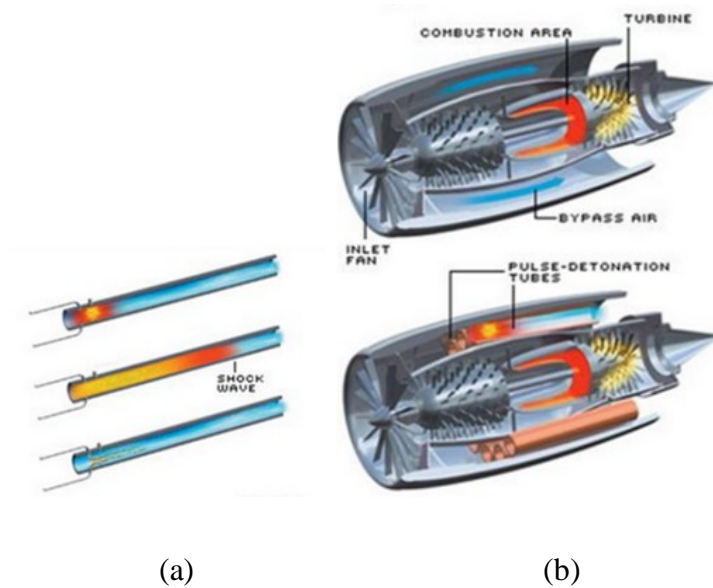


Figure 10 PDE- hybrid gas turbine engine (a) detonation wave propagation in tube, (b) placement of detonation tubes

Pure PDEs find applications in propulsion system for missiles, unmanned vehicles, and other small-scale applications. For these applications, pure PDEs have a higher performance at around Mach 1. To further improve the operating efficiency for high Mach numbers, like at Mach 5, a combined cycle PDE is used where, PDEs are added to the flow path of a ramjet or scramjet engines. These engines would then be suitable for high-altitude, high-speed aircrafts.

Therefore, due to the many advantages offered by PDEs, they can be used in space propulsion systems to reduce the cost and complexity of launching space-crafts.

1.4 Literature Review

1.4.1 Reviews on Experimental Studies

Several studies have been conducted over many decades by various organizations and research facilities in an effort to overcome the shortcomings of using PDE technology. Early in the 1960s, studies were carried out by University of Michigan (Krzycki, 1962) and the US Naval Ordinance Test Station, but they were unable to generate a successful detonation. The reason being inappropriate implementation of a DDT augmentation device. This led to the conclusion that PDEs hold no future for flight applications and further studies came to a halt. However, in 1980s PDE gained attention again due to series of successful experiments carried out by Helman (Helman, June 1986) at the US Naval Postgraduate School. The focus of these studies was to improve the operating frequency and specific impulse. A mixture of ethylene-air was used and based on the experimental results, high operating frequencies of 150 Hz and high specific range of 1000-1400 seconds were obtained.

Further experimental studies done on PDEs were either single-pulse or multi-pulsed detonation based experiments. Single-pulsed experiments involve only the initiation of detonation wave and its propagation followed by blowdown process. Experiments including multi-cycle initiation include the additional purging and refilling processes. Single pulse initiation experiments are carried to determine the required fuel/oxidizer mixture detonation initiation energy, validate the concepts, to measure detonation wave parameters, and to serve as initial stage for more complex multi-cycle initiation. Both hydrogen (H_2) and hydrocarbon based fuels are used in the experiments. The hydrocarbon fuels include both gaseous fuels like ethylene (C_2H_4) and propane (C_3H_8) and liquid fuels like JP10 ($C_{10}H_{16}$). (Ma, 2003)

The performance of a PDE is generally measured based on impulse generated and the process implied for detonation initiation. However, the methods used for impulse measurements fail to be accurate as the engine inlet conditions along with purging and refilling cycles are not considered. Detonation is attained either through direct initiation or DDT (Section III). Through many attempts it is observed that direct detonation is limited to single-pulse experiments, thus most PDE experiments use a DDT process. A proper detonation is achieved based on DDT length which is the distance from the ignition to the detonation formation and it depends on the fuel mixture used, tube dimensions, the tube wall surface roughness and the ignition method used. (Ma, 2003)

Experimental studies carried out by Sinibaldi (Sinibaldi, July 2001) revealed that the placement of ignitor from head end of tube as well as the equivalence ratio for a mixture of $C_2H_4/O_2/N_2$ greatly affects the DDT length. The minimum DDT length of 7.5 cm for the mixture was obtained with an equivalence ratio of 1.2. It was also observed that DDT length increased greatly with a reduced equivalence ratio (ϕ) of 0.75. Similar studies made, lead to the fact that DDT length can be larger compared to actual detonation tube length. Various tests carried out by Hinkey (Hinkey, July 1995) using H_2-O_2 mixtures with different equivalence ratios, suggested employing DDT augmentation devices to attain an affective DDT process with reduced DDT length

To assist in the DDT process, the Shchelkin (Shchelkin, 1940) spiral device is used, introduced by a Russian physicist. Kirill Ivanovich Shchelkin in the year 1965. Based on results of experiments it is found that Shchelkin spiral reduced the DDT length by a factor of about three. Other obstacles were also introduced by various researchers for the same propose. However, it was observed that introduction of these obstacles resulted in total pressure loss and low propulsive

efficiency. As per Cooper (Cooper M. J., 2002) it was reported that the DDT length reduced by 65% but resulted in reduced impulse by 25%.

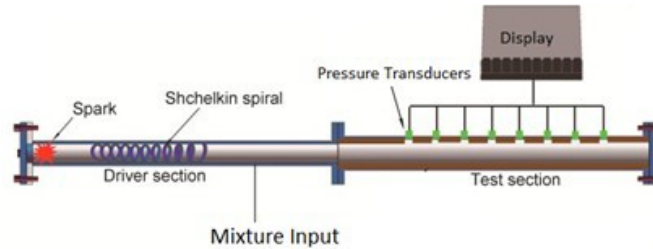


Figure 11 General PDE experimental setup with Shchelkin spiral

A nozzle is used at the end of detonation tube to improve the performance of the PDE by utilizing the internal energy of the exhausting detonation products. However, as PDEs are unsteady by nature it is complicated to design a suitable nozzle. Furthermore, to date, no theory for PDE nozzle design has been established several experimental and numerical studies are reviewed to understand the effects of nozzle design on PDE performance. (Cooper M. a., July 2002)

Experiments carried out by US Naval Postgraduate school (2010) (Kailasanath K.) were focused on increasing the overall efficiency of PDE by converting thermal energy into kinetic energy. This was attained by dynamically varying the effective nozzle area ratio. Testing was conducted on various injection flow rates and computer simulations were also used to observe the fluid flow characteristics. It was observed that mass flow rate injection greatly affected the pressure. However due to insufficient time the experiment was not completed. Another work, carried out by Chen and Fan (2011) (Kailasanath K. , 2009-631) showed the nozzle effects of various shapes on thrust and inlet pressure of a multi-cycle air-breathing PDE. It was observed that

thrust augmentation of a straight nozzle, diverging nozzle and converging-diverging nozzle were better than a converging nozzle. Pressure near the thrust wall increased with addition of nozzle.

It has also been observed through various experiments that flame acceleration, DDT, and detonation propagation is affected greatly by structure and wall roughness of the detonation tube. The velocity of detonation wave is reduced in rough wall tubes as compared to smooth wall tubes (Kailasanath K.) (Kailasanath K. , 2009-631) (Ma, 2003).

Large experimental data from all over the world has provided the effect of various mixture composition of fuels on performance of PDE. Detonations in heterogeneous mixture and having high equivalence ratio, i.e. high fuel concentration, achieved high detonation velocities (Kailasanath K.) (Kailasanath K. , 2009-631).

The tube diameter also affects the propagation of detonation wave. Through experimentally and computational analysis it was found that detonation cell size is a function of initial pressure, temperature, mixture composition and tube diameter (Nichollas, 1957). This is referred to as the critical diameter of the tube. It was concluded that there is successful transition of detonation wave from ignition tube to main combustor tube if the ignition tube diameter is less than the critical diameter. (Cooper M. J., 2002) (T. & G., 1995) (Krzycki, 1962) (Ma, 2003)

Experimental studies have also been carried out to observe the effects of varying the cross sectional area of the detonation tube. In doing so, the transient behavior of the propagating shock and the subsequent flow characteristics were predicted. These studies included keeping the same tube diameter, or maintaining the same diaphragm pressure ratio, and by introducing tapering a section of the channel. It was observed that the strength of the shock wave (its velocity, detonation pressure and so on) travelling down a channel of varying area, was affected positively or negatively

depending upon the tube area at that location, as well as the flow behind the shock were disturbed. However, not many studies have been carried out, to predict the exact behavior of the shock waves.

The above mentioned experimental studies have many limits and hence numerical or computational modelling is generally preferred to study the unsteady nature of PDE.

1.4.2 Reviews on Computational Modeling Studies

Various numerical and analytical investigations were made to attain a better understanding of single-pulse and multi-pulse operations of various single tube or multi-tube PDEs in combination with and without nozzles and ejectors.

To estimate the performance of PDEs, a simple model was proposed by Endo and Fujiwara. (Endo & Fujiwara, 2002) The model consists of a straight tube, closed at one end (inlet) and open on the other end (outlet), having a detonation region near the closed end and does not include a nozzle at the outlet. The one cycle pulse consists of three phases: combustion, exhaust, and filling phases. The simulations carried out on this model showed that through simplified theoretical analysis, useful formulae for impulse density per unit cycle operation and time-averaged thrust density could be derived.

Analytical studies undertaken by Yungster (Yungster, 2003) to understand the effects of adding nozzle at exhaust of detonation tube. A numerical model was setup and computational fluid dynamics was used to confirm results. Single pulsed simulations for a 1.0 m long tube with or without nozzle filled with hydrogen-air mixture. Multi-cycle analysis results showed that the combustion products need to be purged from nozzle before start of next cycle, for nozzle to function effectively **Figure 12**.

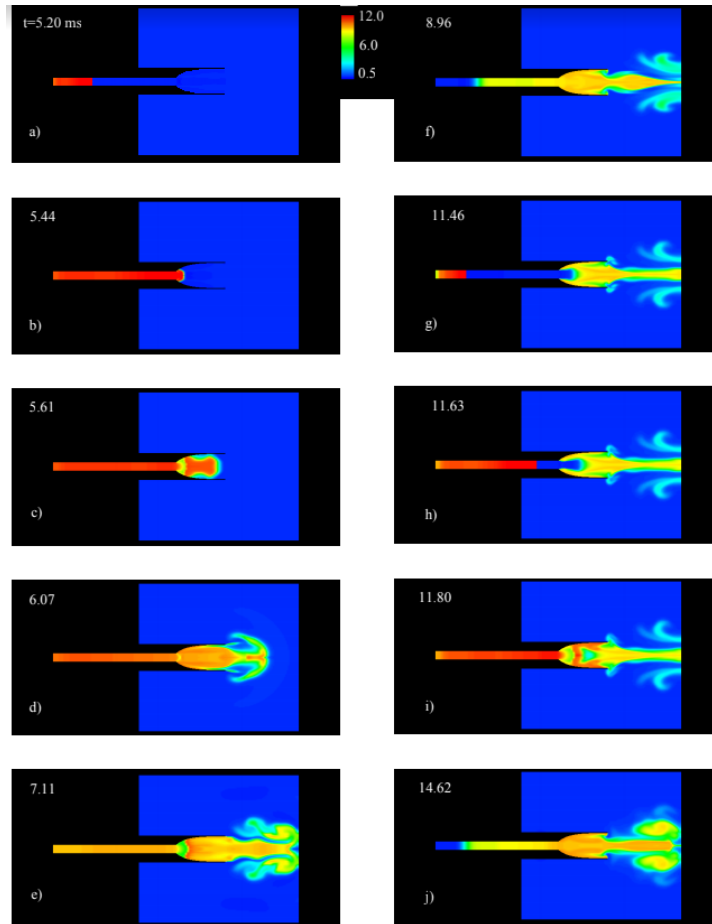


Figure 12 Multi-cycle simulations showing temperature contours

One of the main challenges of producing PDEs practically, is the requirement for repeated initiation of detonations within a detonation chamber. The requirement to capture the time-accurate motion of a detonation wave is a challenge in computational modelling. Shihari, Mallesh et al. (Shihari & Mallesh, 2015) studied the one-step overall reaction model to reduce this computational load. Both 1-D and 2-D axisymmetric tubes were considered for simulations. Their studies showed that a one-step model is sufficient to predict the flow properties. They also investigated the influence of different grid sizes on the occurrence of a von Neumann spike, CJ pressure, and detonation velocity.

Ma (Ma, 2003) conducted CFD simulations to study flow dynamics and system performance of air-breathing PDEs using H₂-air one step reaction model. The simulation model consisted of supersonic inlet, an air manifold, a rotary valve, a single or a multi-tube combustor, and a convergent-divergent nozzle at predefined flight conditions. It was observed that keeping purge time constant with longer refilling cycles, increased the specific thrust and C-D nozzle increases the propulsion efficiency as the throat area plays a more important role than tube length. It was also noted that multi-tube PDEs improve operational steadiness of the system compared to single-tube geometry. This geometry helps reduced the imperfect nozzle expansion loss, however, it induces more complicated shock waves and internal flow loss, thus decreasing the overall propulsive performance.

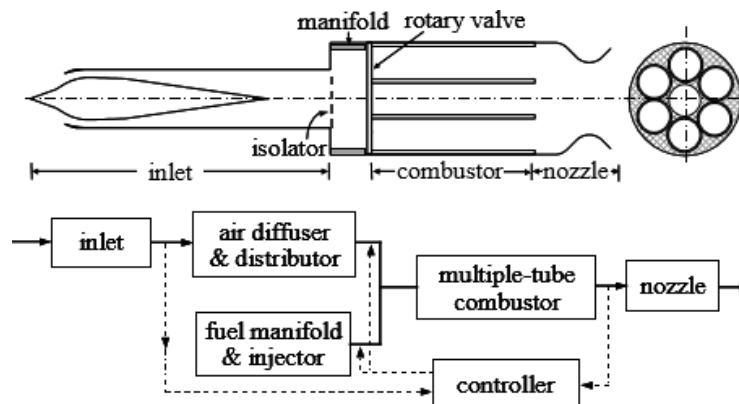


Figure 13 Schematic of supersonic air-breathing PDE

It is necessary to study the intake flow analysis of PDE, as this significantly affects the combustion process and hence the thrust generated. Unsteady flow within the intake system of a hydrogen-air PDE was analysed by Strafaccia and Paxson (Kailasanath K. , 2009-631) using a quasi 1D CFD code. The effect of fill fraction was better understood using an inlet model with single fuel injector. The computed results showed that at constant fuel mass flow rate injection

creates large local variations in equivalence ratio throughout the PDE cycle and it was suggested to maintain the fill ratio of 1.0 to avoid any loss of thrust.

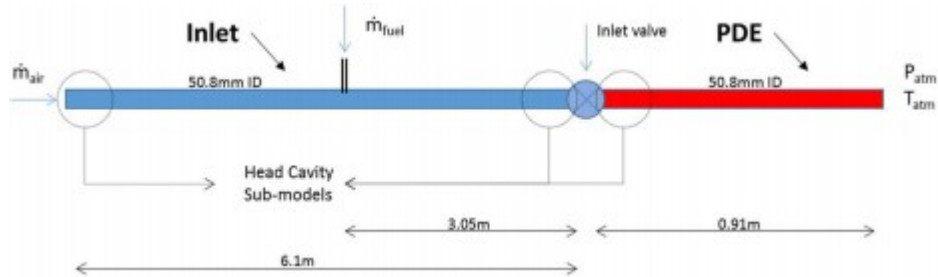


Figure 14 Computational PDE model with dimensions (including choked inlet, intake tube, and constant fuel mass flow)

Another study on the effects of the flow intake was conducted by Ma and Choi (Vizcaino, 2013) by modeling and simulating a valve-less air-breathing PDE. It was also being experimentally developed and studied at U.S. Naval Postgraduate School. Using an ethylene/oxygen/air mixtures the entire flow dynamics and multi-cycle operation of the engine was carefully investigated. Their results indicated that the inflow must be carefully monitored to ensure successful propagation of detonation wave from the initiator to main combustion chamber.

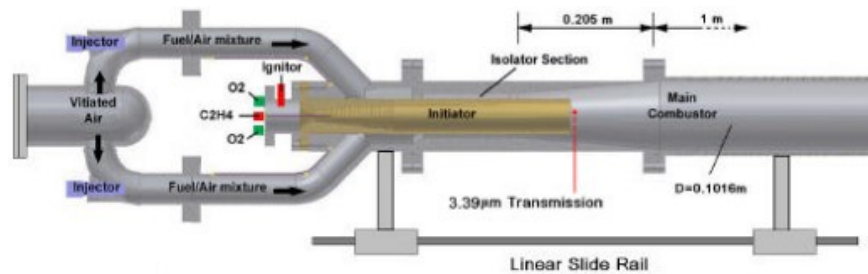


Figure 15 Schematic of a Valve-less PDE setup

The stoichiometry of the propellants used, significantly effects the simulation results. A study carried out by Ebrahimi and Merkel (Ebrahimi, 2002) demonstrates the operational

performance of PDE based on the chemical reaction rate and number of species in CFD model. 1D and 2D, transient calculations were employed assuming finite rate chemistry for hydrogen/oxygen combustion, based on eight chemical species and 16 reactions. Results indicated variations in thrust and specific impulse as well as elevated chamber wall temperatures (approximately 1500 K) for multi-cycle simulations.

In terms of applications of PDE, Harris and Stowe (Kailasanath K.) performed a system-level performance analyses of a PDE as a Ramjet replacement for Mach 1.2 to 3.5. With the help of a two-dimensional constant volume analytical model, detonation timing, geometric and injection parameters, providing optimal performance were determined. They also evaluated the effect of partial fill and nozzle expansion ratio on specific impulse. It was observed that for the considered Mach numbers, specific impulse for PDE was greater than that of a ramjet.

Recent studies are being carried out on PDE-hybrid gas turbine. CFD investigation carried out by General Electric Global Research Centre, NY; studied the PDE-turbine interactions with PDE operation on H₂- air located upstream of one row of stationary, 2D turbine blades. The result showed that the system reached a quasi-steady state rapidly for multi-cycle simulations than a single pulsed, thus highlighting the limitations of single cycle calculations (Ma, 2003).

A computational and experimental program undertaken by Combustion Sciences Branch of the Turbine Engine Division of the Air Force Research Laboratory focus on developing a PDE model that uses a commercial available fuel (kerosene based, like the JP10). Preliminary data is being obtained with premixed hydrogen- air mixture (Hinkey, July 1995).

From the literature review on computational analyses it is seen that none of the models proposed have attempted to represent the unsteady flow in a tube having converging or diverging

tube geometry. Generally, performance estimates of PDEs is done using an idealized straight detonation tube without inlets or any other additional apparatus. The study of ZND conditions are then studied as the wave propagates along the length of tube till the open end. It is not entirely possible to perform a direct comparison between the simulated results and experimental data as the effects of factors such as initiators used and the boundary conditions applied differ.

1.5 Project Proposal

Study of PDEs has been a challenge to engineering knowledge by pushing the boundaries of gas dynamics and help gain better understanding of combustion science and fluid dynamics. A great part of current PDE research seems to be aiming at making the engine more commercially applicable. As PDEs have a simple structure, accurate performance estimations on them can be done by methods of CFD.

The objective of this project is to initially model a detonation flame front and successfully run a single-tube pulse detonation engine using available CFD software. In doing so the time-accurate motion of detonation wave will be captured using a finite rate chemistry. Once successful, the effects of converging or diverging tube geometries on detonation propagation will be studied.

1.6 Methodology

For this study, initially an ideal PDE tube will be modeled to observe the ZND conditions in 1D detonation wave propagation. The setup will be simulated considering one-step chemical reaction model for hydrogen-air mixture. The CFD will be modeled using available version of ANSYS FLUENT. The fluid mechanisms for PDE performance will be determined mainly for a laminar viscous flow model. The heat-conduction, radiation and acoustics effects will not be considered. The 2-D axisymmetric Euler equations for a multi-species, thermally perfect, chemical

reacting gas is taken into account where the global conservation equations are replaced by addition of chemical species. On obtaining the desired results for this model, the tube will be converged or diverged by introducing a positive or negative inclination, to study the effects on detonation propagation.

CHAPTER 2 COMPUTATIONAL ANALYSIS SETUP

2.1 Detonation Initiation

In order to start the PDE cycle stated in previous chapter; detonation initiation is achieved via direct detonation initiation or deflagration-to-detonation transition (DDT).

2.1.1 Direct Initiation

The direct initiation is started by providing energy to the closed end of the tube. The mechanism for this type of detonation initiation is specific to the type of ignition source used. This type of detonation initiation provides a constant velocity propagation inside a short length tube. However, this require huge amount of energy which further reduce the engine efficiency. (Lee, 2008) (Garg & Dhiman, October, 2014).

In this paper, the detonation will be achieved through direct initiation. For this a high pressure and a high temperature gas is introduced in the narrow region next to the closed end of the tube.

2.1.2 Deflagration to Detonation Transition (DDT)

For a deflagration based initiation, it is hard to achieve a constant velocity propagating wave as upon ignition, the self-propagating deflagrations tend to accelerate continuously and thus are intrinsically unstable. However, by applying the appropriate boundary conditions the subsonic deflagration is accelerated to a supersonic detonation velocity, thus transitioning abruptly between two distinct states (Lee, 2008). With the help of a small ignition the deflagration is created and the transition process then takes several meters of the detonation tube length and a corresponding large amount of time, which can limit life frequency. This is in contrast to a direct initiation (Section 2.1.1). Thus, the DDT process can be divided into four phases: Deflagration initiation, flame

acceleration, formation and amplification of explosion centers, and formation of a detonation wave.

2.3 Chemical Kinetics

In order to get the desired detonation going, it is necessary to introduce the accurate amount of fuel-oxidizer ratio. This required amount is determined based on the equivalence ratio ϕ which is defined as the actual fuel-oxidizer ratio to the chemically reacted fuel-oxidizer ratio. The equivalence ratio can be calculated using either the mass fraction or the mole fraction of the components or species of a given chemical equation as follows (Lim, 2010-12);

$$\text{Mass fraction } Y = \frac{m_{fuel}}{m_{oxidizer}} \text{ and Mole fraction } N = \frac{\eta_{fuel}}{\eta_{oxidizer}}$$

$$\phi = \frac{Y_{actual}}{Y_{chemically\ reacted}} = \frac{N_{actual}}{N_{chemically\ reacted}}$$
(2.1)

Based on the above equation if value of ϕ is more than one it implies that the mixture is fuel rich and less than one or just one, it implies that the mixture is fuel lean. Thus, the value of equivalence ratio influences the thermodynamic properties and composition of the fuel-oxidizer during the process of detonation. Because of its effects in achieving better ZND conditions, a mixture of hydrogen-air having equivalence ratio (ϕ) of 1.0 is used for chemical combustion.

For this paper a one-step reaction model is considered. A one- or a single-step reaction model is defined as the chemical reaction in which one or more chemical reactant species undergoes chemical change to form products in a single reaction step with a single transition state. The following equation gives this one step reaction.



Calculations of Mass Fraction for equation 2.2

For $\phi = 1.0$ the species mass fractions (λ) for reactants and products are calculated as;

Reactant Species:

$$Y_{H_2} = \frac{2H_2}{2H_2 + (O_2 + 3.76N_2)} = \frac{2(2.01588)}{2(2.01588) + (31.998 + 3.76(28.0134))} = 0.02852$$

$$Y_{O_2} = \frac{O_2}{2H_2 + (O_2 + 3.76N_2)} = \frac{31.0998}{2(2.01588) + (31.998 + 3.76(28.0134))} = 0.22635$$

$$Y_{N_2} = \frac{3.76N_2}{2H_2 + (O_2 + 3.76N_2)} = \frac{3.76(28.0134)}{2(2.01588) + (31.998 + 3.76(28.0134))} = 0.74512$$

Products Species

$$Y_{H_2O} = \frac{2H_2O}{2H_2O + 3.76N_2} = \frac{2(18.0152)}{2(18.0152) + 3.76(28.0134)} = 0.25488$$

$$Y_{N_2} = \frac{3.76N_2}{2H_2O + 3.76N_2} = \frac{3.76(28.0134)}{2(18.0152) + 3.76(28.0134)} = 0.74512$$

The above calculated values will then be used as initial species input values for the direct initiation CFD setup. Default available ANSYS FLUENT values of pre-exponential factor and activation energy are chosen for the present study ($A_r = 9.87 \times 10^8$, $E^+ = 3.1 \times 10^7$ [J/kg-mol]).

2.4 Converging and Diverging Detonation Tube Geometries

Generally, a simple detonation tube consists of a flow channel having a constant rectangular area, closed at one end and open to the atmosphere at the other. Due to the detonation process, the velocities generated are of the magnitude 2000 [m/s], thus leading to a supersonic or a hypersonic flow in the tube.

As per the compressible flow theory for a 1-D supersonic flow ($M > 1$), an increase in flow velocity is attained with an increase in the area of the channel (Anderson, 2015). Likewise, a decrease in the flow velocity is associated with decrease in the area of the channel. The relation is represented as:

$$\frac{dA}{A} = (M^2 - 1) \left(\pm \frac{du}{u} \right) \quad (2.3)$$

Where,

dA = change in tube cross sectional area, (A = cross sectional area of the tube)

du = change in the flow velocity, (u = flow velocity)

(+ = increase and - = decrease)

Thus, for a supersonic flow, to increase the velocity, a divergent area is introduced, and to decrease the velocity, a convergent area is introduced in the flow channel.

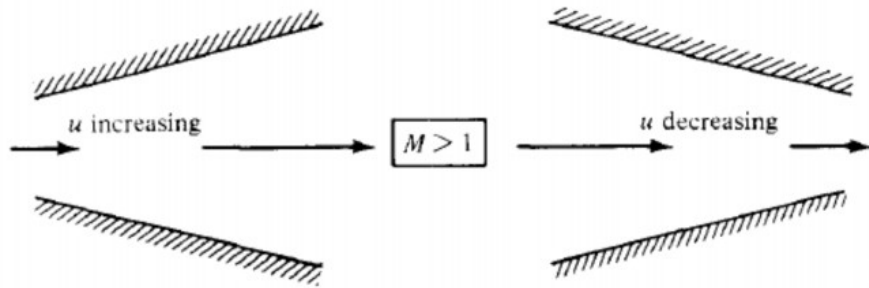


Figure 16 Supersonic Flow in Converging -Diverging Section

A similar effect can be studied in the rectangular detonation tube by tapering a section of the tube upwards or downwards, thus diverging or converging near the exit of the tube. This can be done by keeping a portion of the tube as a constant area and then introducing a sudden increase or decrease in the tube area, or gradually introducing a tapering from the closed end of the tube.

So far, there has not been published to date, any experimental or numerical justification of the effects of converging-diverging sections in an unsteady flow.

2.5 Boundary Conditions Setup

As per the literature review, to correctly simulate the detonation propagation it is needed to setup appropriate boundary conditions. The closed end and the upper side of the tube is considered as 'wall'. The lower side of the tube is set as 'axis' or 'wall' as per the simulation requirement. The open end is generally considered as a 'pressure outlet', set at standard atmospheric conditions (Yungster, 2003).

2.6 CFD Solver

The solver for CFD is included in Setup for ANSYS FLUENT, where the physics of the problem is defined and solution is converged. A 2-D double precision solver is used to provide accuracy for long tube PDE geometry. There are two kinds of solvers available in FLUENT:

Pressure-based solver and Density-based coupled solver. A density based solver is chosen for simulation as it is applicable when there is a strong coupling, between the equations of state and/or species. This solver solves the governing equations for mass, momentum, energy and species transport simultaneously by employing a finite volume discretization method. Pressure is obtained through the equation of state. Several iterations are needed to be performed to converge the solution as the governing equations are coupled and non-linear. (Gopalakrishnan, 2017)

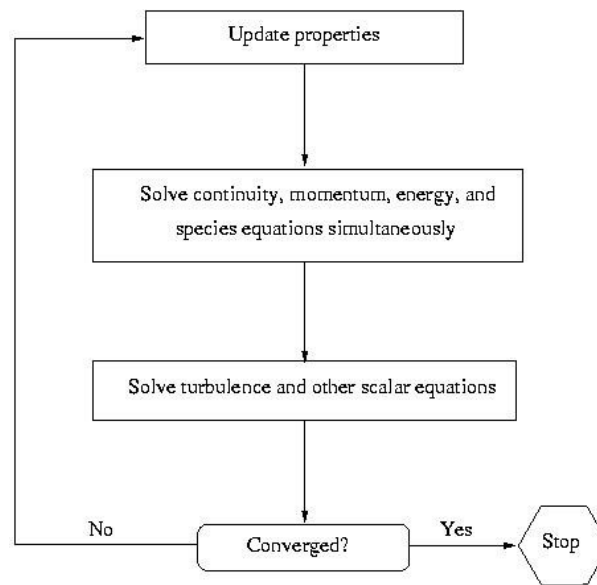


Figure 17 Algorithm for Density Based solver in ANSYS Fluent

The density-based solver can use either an implicit or explicit solution approach. Implicit formulation is selected as the variables in all computational cells are solved simultaneously and solution converges faster. However, this method takes more computation time and memory than explicit approach. Roe’s Flux- Difference Splitting (Roe-FDS) scheme is recommended for high Mach number flows as this scheme admits shocks as a possible solution of Euler equations, without any extra calculations efforts. (Gopalakrishnan, 2017) (FLUENT, 2017)

Several computational analyses were performed on an ideal PDE model to achieve the desired ZND model parameters. Through literature reviews it was observed that ANSYS Fluent (FLUENT, 2017) is capable of handling detonation generation. Hence, it has been chosen for simulating an ideal PDE tube and calculating CJ and ZND detonation conditions. At the time of performing CFD analysis the version ANSYS Fluent 19.1 is being used due to its availability. A case study for 1-D detonation propagation with one-step chemical reaction model will be done to verify the software's capability.

CHAPTER 3 GOVERNING EQUATIONS

The computational analysis of a problem in fluid dynamic is done in three steps: (i) model a computational domain in the fluid, (ii) apply the conservation equations to this domain to exemplify the physics and (iii) use these equations to get desired solutions. In Chapter 1 a background study on PDE theory and concept was provided. This chapter deals with the governing equations used for solving an ideal PDE model through computational analysis.

The system of governing equations used in ANSYS FLUENT to calculate the mean flow properties for an arbitrary control volume V having a differential surface area $d\mathbf{A}$ as follows (FLUENT, 2017):

$$\frac{\partial}{\partial t} \int_V \mathbf{W} dV + \oint [F - G] d\mathbf{A} = \int_V \mathbf{S} dV \quad (3.1)$$

Where the vectors \mathbf{W} , \mathbf{F} , and \mathbf{G} are defined as follows:

$$\mathbf{W} = \begin{matrix} \rho \\ \rho u \\ \rho v \\ \rho w \\ \{\rho E\} \end{matrix}, \mathbf{F} = \begin{matrix} \rho v \\ \rho v u + p \hat{i} \\ \rho v v + p \hat{j} \\ \rho v w + p \hat{k} \\ \{\rho v E + p v\} \end{matrix}, \mathbf{G} = \begin{matrix} 0 \\ \tau_{xi} \\ \tau_{yi} \\ \tau_{zi} \\ \{\tau_{ij} v_j + \mathbf{q}\} \end{matrix} \quad (3.2)$$

The source terms such as body sources and energy sources are denoted by the vector \mathbf{S} . Here, ρ , v , E , p , τ , and \mathbf{q} represent the density, velocity, total energy per unit mass, static pressure of the fluid, viscous stress tensor, and the heat flux respectively. Total enthalpy H and the total energy E is given by,

$$H = h + \frac{|v^2|}{2} \quad (3.3)$$

And

$$E = H - p/\rho \quad (3.4)$$

PDEs are generally modeled as 2-D axis-symmetric and when applying the assumptions made for the transient combustion process in a pulse detonation tube, the governing equations simplify to the unsteady 2-D Euler equations (Rouf, 2003), neglecting the vector \mathbf{G} .

For modeling of chemical reactions, a one-step overall irreversible Arrhenius kinetics is used, resulting in source terms being added. Furthermore, this results in following equations expressed as (Srihari & Mallesh, 2015):

$$\frac{\partial \mathbf{W}}{\partial t} + \frac{\partial \mathbf{F}_u}{\partial x} + \frac{\partial \mathbf{F}_v}{\partial y} = \mathbf{S} \quad (3.5)$$

$$\mathbf{W} = \begin{matrix} \rho \\ \rho u \\ \rho v \\ E \\ \{\rho\lambda\} \end{matrix}, \mathbf{F}_u = \begin{matrix} \rho u \\ \rho u^2 + p \\ \rho uv \\ (E + p)u \\ \{\rho u\lambda\} \end{matrix}, \mathbf{F}_v = \begin{matrix} \rho v \\ \rho uv \\ pv^2 + p \\ (E + p)v \\ \{\rho v\lambda\} \end{matrix}, \mathbf{S} = \begin{matrix} 0 \\ 0 \\ 0 \\ 0 \\ \{\dot{\omega}\} \end{matrix}$$

(3.6)

Where E is now written as;

$$E = \frac{p}{(\gamma - 1)\rho} + \frac{\rho(u^2 + v^2)}{2} + \rho p \lambda \quad (3.7)$$

The pre-mixed test gas mixtures are considered and the burned gas is isentropically expanded. The source term for species equation is given as a function of Arrhenius coefficient Ar and activation energy E^+ ;

$$\dot{\omega} = -Ar \exp\left(-\frac{E^+}{RT}\right) \rho \lambda \quad (3.8)$$

This approach completely neglects any turbulence disturbances and considers only the effects of chemistry.

In the ZND model for detonation, it is assumed that: (i) the flow is one dimensional; (ii) the heat conduction, radiation, diffusion, and viscosity are neglected; (iii) there is no reaction occurring ahead of the shock and thus the reaction rate is considered null; (iii) a one-step, irreversible, finite rate chemical reaction; and (v) all thermodynamic variables except the chemical composition are in local equilibrium state (Thattai, 2010). Therefore, the two dimensional Euler equations for ZND model are used.

As, the general governing equations form a set of coupled, non-linear partial differential equations, it is not possible to solve these equations numerically for most engineering problems. However, it is possible to get approximate computer-based solutions to these equations through computational fluid dynamics (CFD) by making many assumptions. Considering the goals of the present study, the proper selection of flow solver must be made. In addition, the solver should be able to simulate a detonation wave and model detailed chemical reactions.

CHAPTER 4 CASE VALIDATION: EFFECTS OF TUBE GEOMETRY

4.1 Case 1: 1-D Wave Propagation in a Constant Area Tube

In the present computational simulation, the tube having a length (L_t) of 0.75 [m] and a diameter (D_t) of 0.073 [m] is selected based on literature review. The direct detonation initiation area is placed 0.005 [m] from the head end tube. This geometry used is generally referred to as an ideal, 2-D axisymmetric model (Figure 18).

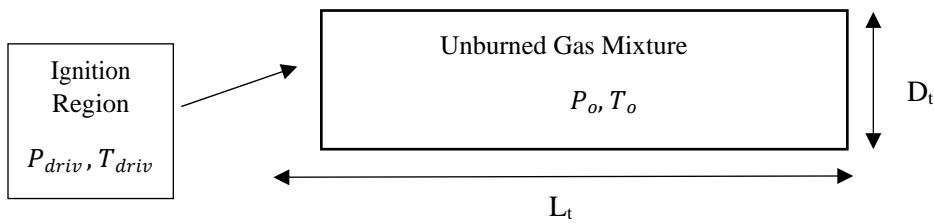


Figure 18 Schematic of 2-D Axisymmetric Ideal PDE tube

A simple structured adaptive mesh with 2-D grids of size 0.1 [mm] is used to better estimate the flow and detonation properties developing inside PDE tube (Figure 19).

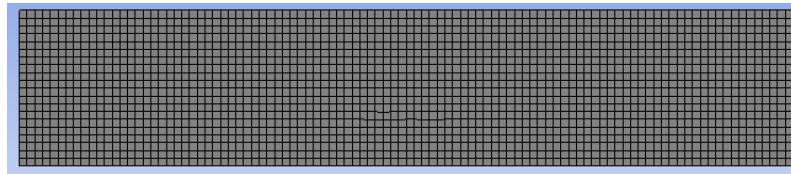


Figure 19 2-D Adaptive mesh of ideal PDE tube

The model is initialized by patching the thin detonation region with steam (H_2O) and nitrogen gas at high pressures and temperatures while the hydrogen-air mixture was patched in remainder of the tube having standard atmospheric conditions (Figure 18) (Figure 20). The following tables, Table 1 and Table 2 show the initial conditions for both the regions. The calculations for mass fraction of each species is as per Chapter 2, Section 2.3 (Lim, 2010-12) (Vizcaino, 2013).

Table 1 Setup and initialization conditions unburned gas mixture

Input Parameters		Values
Initial Pressure	P_0	1 [atm]
Initial Temperature	T_0	300 [K]
H_2 Mass Fraction	λ_{H_2}	2.852 %
O_2 Mass Fraction	λ_{O_2}	22.635 %
N_2 Mass Fraction	λ_{N_2}	74.512 %
H_2O Mass Fraction	λ_{H_2O}	0.000 %

Table 2 Setup and initialization conditions for ignition region

Input Parameters		Values
Initial Pressure	P_{driv}	30.4 [atm]
Initial Temperature	T_{driv}	3000 [K]
H_2 Mass Fraction	λ_{H_2}	0.000 %
O_2 Mass Fraction	λ_{O_2}	0.000 %
N_2 Mass Fraction	λ_{N_2}	74.512 %
H_2O Mass Fraction	λ_{H_2O}	25.488 %

The time step size was set to 10^{-8} seconds as the reaction time for detonation is very small. Courant-Friedrichs-Lewy (CFL) number was reduced to 0.5 based on the small grid size. As no turbulence was considered, the viscous model is set to laminar.



Figure 20 Initial conditions for the ideal PDE tube with pressure contour

The simulation of the reaction model is compared with Vizcaino as the gas mixture used was hydrogen-air and 2-D axisymmetric simulation was done using ANSYS Fluent code. Although for his simulation, nitrogen was treated as an inert gas i.e. non reacting species, for this model nitrogen is included in the reaction model for attaining better ZND conditions.

4.2 Case 2: 1-D Wave Propagation in Varying Area Tube

For the varying area, the PDE tube is inclined at angles $\alpha = +1^\circ, +2^\circ, +3^\circ$ and $-1^\circ, -2^\circ, -3^\circ$ (Figures 21 and 22). This inclination, positive or negative, is introduced in the unburnt gas mixture section of the tube, keeping the length (L_i), the diameter at the closed end of the tube, and the area of the ignition region constant having values as mentioned in Section 4.1. Thus, only the diameter of the open end varied as per the inclination angle (α). This geometry set-up is modeled for a 2-D axisymmetric simulations.

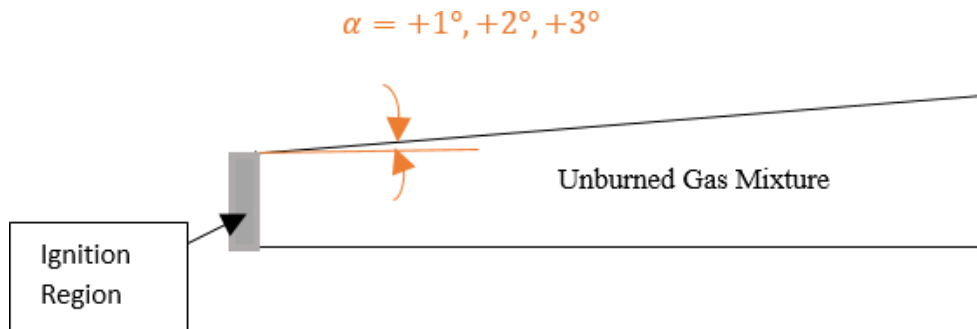


Figure 21 PDE tube with positive angle of inclination (α)

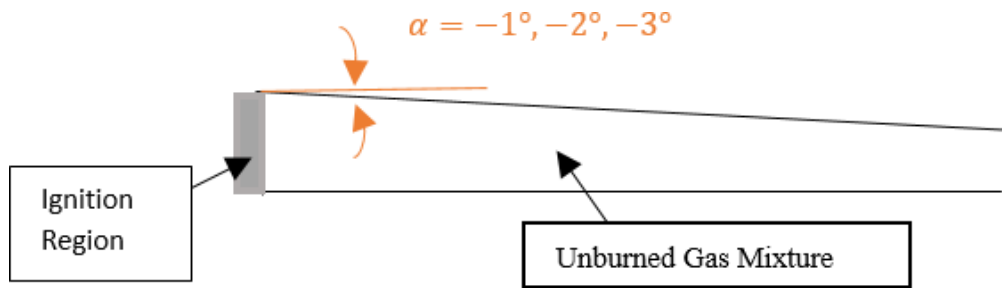


Figure 22 PDE tube with negative angle of inclination (α)

The initial conditions used for the detonation of this inclined tube are similar to those used in Case 1. At the time of writing this report, the author was unable to find any established data to support the results obtained.

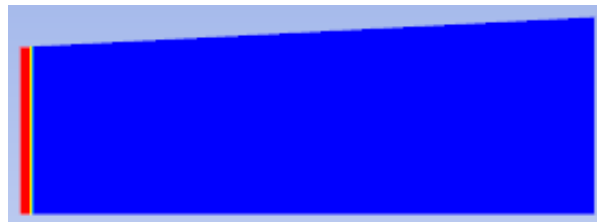


Figure 23 Initial conditions for PDE tube having positive inclination with pressure contour



Figure 24 Initial conditions for PDE tube having negative inclination with pressure contour

CHAPTER 5 RESULTS AND DISCUSSION

5.1 Constant Area Rectangular Tube

Figure 25 shows the pressure evolution of the detonation wave as it travels along the length of the tube after the detonation is initiated from the head end of the tube. As the detonation matured along the length of the tube, certain CJ and ZND trends started to emerge. These generated outcome is then compared with benchmark literature.

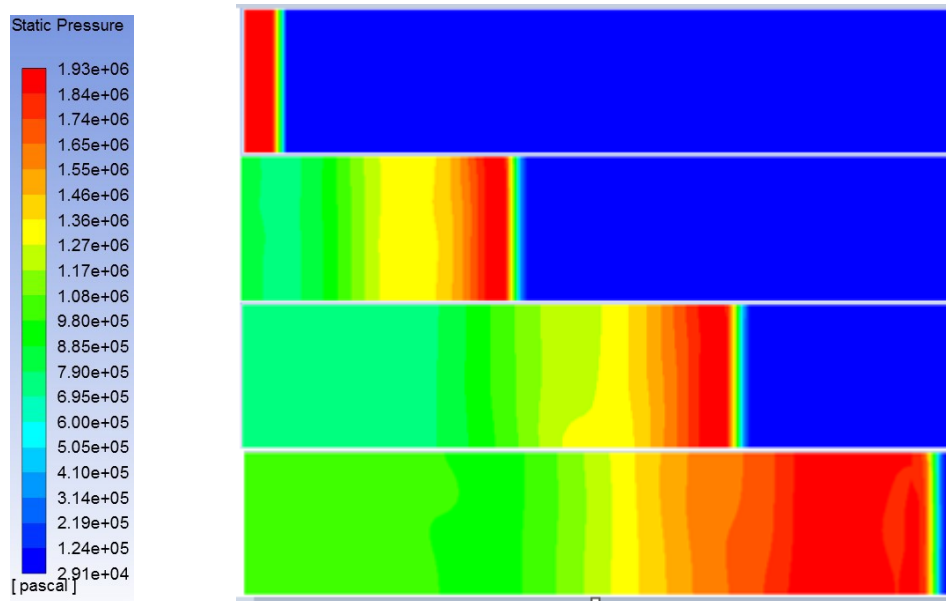


Figure 25 Detonation wave propagation along the ideal PDE tube with Pressure contours

Pressure

For a lean mixture of hydrogen-air, the passage of the initial detonation pressure spike rise occurred at 0.01 [mm] from the head end of the tube. This von Neumann spike pressure remained around 27.23 [atm] before rapidly trailing off. This pressure spike indicates the maximum reaction rate occurring at that location. However, this spike value observed is higher than the Vizcaino (Vizcaino, 2013) model. The following figure displays the pressure distribution yielding ZND

model characteristics. It can be observed how the induction and reaction zones dramatically affects the pressure in the region of burned gas.

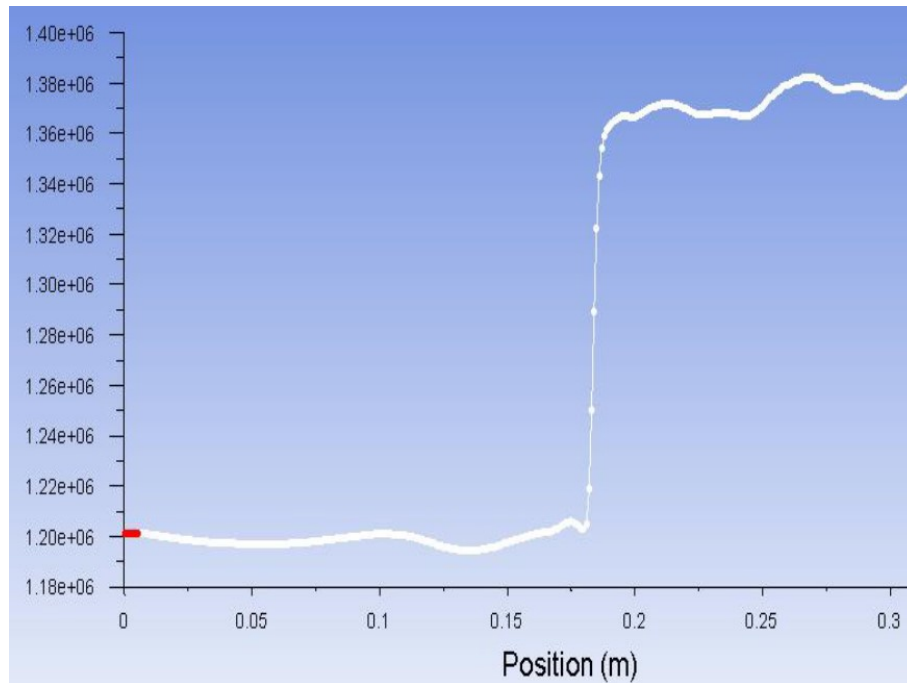


Figure 26 ZND Pressure profile

Temperature

The temperature rises sharply to a peak value of 3500 [K] before trailing off to a constant value of 2900 [K], showing similar trend as the pressure distribution. This high value of temperature is observed at position 0.01 [m] from the head end of the tube. The figure below shows the temperature distribution for ZND characteristics affected by the induction and reaction zones.

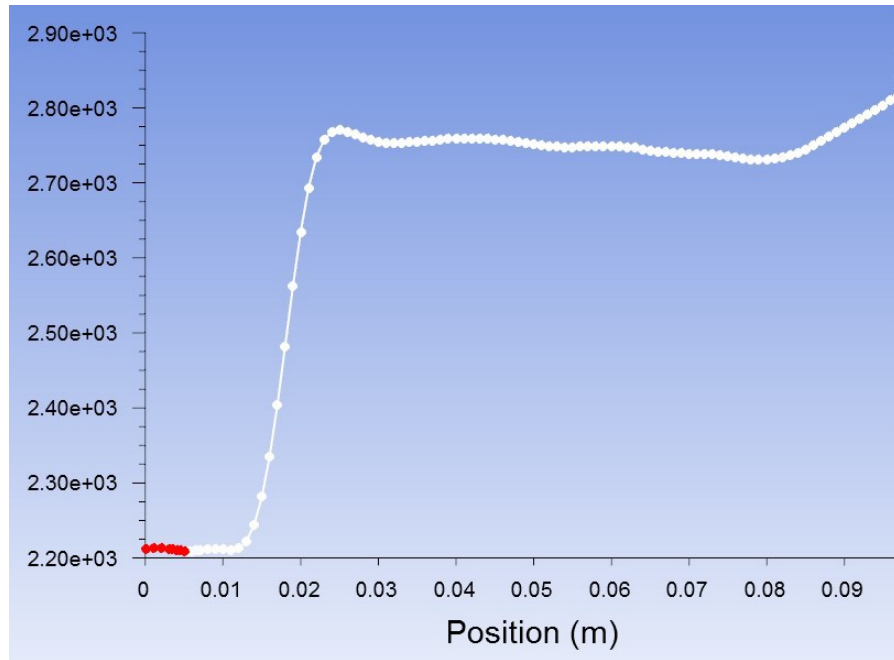


Figure 27 ZND Temperature profile

Thus, it can be concluded that the one-step chemical reaction hydrogen –air mixture can be used to simulate ZND model behavior.

CJ Velocity

CJ velocity is calculated by averaging the wave velocity measured at several different locations. This is done by using simple kinematics where average velocity is displacement over total time elapsed. The displacement values were selected with respect to the position of the peak pressure wave. The resulting average of speeds from 0.1 [m] to 0.6 [m] away from the head end wall was found to be approximately 2200 [m/s] (Table 3). The detonation velocity obtained by Vizcaino (Vizcaino, 2013) is similar to the obtained results.

Table 3 Wave velocity measurement

Distance [m]	Flow Time [s]	Velocity [m/s]
0.1	0.000049	2041
0.2	0.00009	2222
0.3	0.00014	2143
0.45	0.00019	2368
0.6	0.00027	2222
Average		2200 [m/s]

5.2 Simulation vs. NASA CEA

Theoretical detonation parameters were calculated using NASA CEA code (Bonnie & Sanford, 2004) (Appendix C) to verify the simulation results. Hydrogen-air mixture is used with equivalence ratio (ϕ) of 1.0 at standard initial pressure and temperature conditions (input values like those in Table 1). It is observed that the CJ parameters obtained using NASA CEA are comparable with the current obtained values (Table 4).

Table 4 CJ conditions

Detonation Parameters		CFD	NASA CEA
Pressure Ratio at CJ point	P_2/P_1	18.25	15.5
Temperature Ratio at CJ point	T_2/T_1	9.56	9.82
CJ Detonation Velocity	U_{CJ}	Case 1: 2200 [m/s]	1967.6 [m/s]

Comparing the simulations CJ values with theoretical values it was observed that theoretical yields a -17.74 % difference for pressure, 2.71 % difference for temperature, and a -12.19 % difference for detonation velocity. These percentage errors obtained are around the similar values to the ones observed by Vizcaino (Vizcaino, 2013). Figure 26 and Figure 27 shows the variation of physical properties following the ZND detonation trend explained in sections 1.2.4 and 1.2.5, thus further endorsing the results obtained.

5.3 Varying Area Tube

The following figures, Figures 28 and 29, show evolution of the detonation characteristics for a tube having positive and negative inclination. The CJ and ZND trends were noted for each angle of inclination.

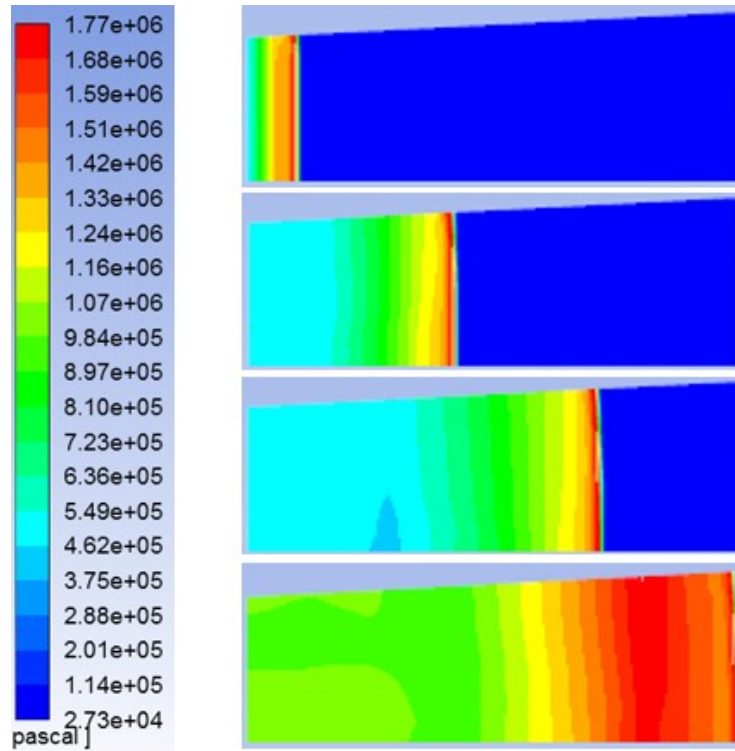


Figure 28 Detonation wave propagation along the PDE tube with positive inclination showing pressure contours

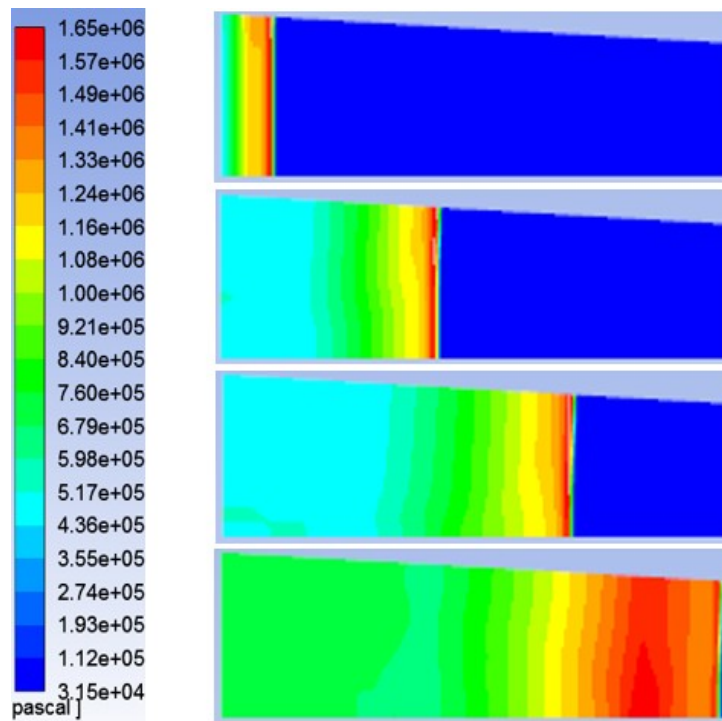


Figure 29 Detonation wave propagation along the PDE tube with negative inclination showing pressure contours

Pressure

The value von Neumann spike pressure and the ZND pressure profile did not show much change from those observed for Case 1, Section 5.1.1. However, it was noted that the value of the detonation pressure decreased with increase in inclination angle (α). The following table shows the comparison in pressure for the straight tube and tube with inclination;

Table 5 Variations of Pressure in PDE tube with inclinations

Angle of inclination (α)	Detonation Pressure [MPa]
No inclination/ straight tube	1.6
-1°	1.65
-2°	1.76
-3°	1.92
+1°	1.55
+2°	1.53
+3°	1.51

Thus, it can be seen that the decrease in pressure occurs when the area of tube is increased, further leading to increase in the wave velocity.

Temperature

Even though, the detonation pressure showed variations with respect to the angle of inclination (α), the temperature profile remained more or less the same. This value was observed to be around 3500 [K] similar to the value observed in Section 5.1.1.

CJ velocity

The CJ velocity is calculated in the similar manner as described in Section 5.1.1. The following tables show the average waveform speed calculated for each angle of inclination.

Table 6 Wave velocity measurement for $\alpha = -3^\circ$

Distance [m]	Flow Time [s]	Velocity [m/s]
0.1	0.0000529	1890
0.2	0.00010	1818
0.3	0.000158	1898
0.45	0.00021	2143
0.6	0.000281	2135
Average		1977 [m/s]

Table 7 Wave velocity measurement for $\alpha = -2^\circ$

Distance [m]	Flow Time [s]	Velocity [m/s]
0.1	0.000052	1923
0.2	0.0001072	1865
0.3	0.0001573	1907
0.45	0.0002073	2171
0.6	0.0002791	2150
Average		2003 [m/s]

Table 8 Wave velocity measurement for $\alpha = -1^\circ$

Distance [m]	Flow Time [s]	Velocity [m/s]
0.1	0.0000504	1980
0.2	0.00009	2000
0.3	0.0001455	2062
0.45	0.0002005	2244
0.6	0.0002755	2178
Average		2093 [m/s]

From the above tables it is observed that the average wave speed decreased from the originally calculated one for a straight constant area tube. Furthermore, it is observed that this waveform speed continues to decrease with decreasing angle of inclination.

Table 9 Wave velocity measurement for $\alpha = +1^\circ$

Distance [m]	Flow Time [s]	Velocity [m/s]
0.1	0.00004	2500
0.2	0.000099	2002
0.3	0.000155	1935
0.45	0.0002	2250
0.6	0.00027	2222
Average		2182 [m/s]

Table 10 Wave velocity measurement for $\alpha = +2^\circ$

Distance [m]	Flow Time [s]	Velocity [m/s]
0.1	0.00004	2500
0.2	0.0000899	2225
0.3	0.00014	2143
0.45	0.000202	2228
0.6	0.000284	2113
Average		2242 [m/s]

Table 11 Wave velocity measurement for $\alpha = +3^\circ$

Distance [m]	Flow Time [s]	Velocity [m/s]
0.1	0.00004	2500
0.2	0.0000849	2356
0.3	0.00013	2308
0.45	0.000195	2308
0.6	0.000275	2182
Average		2331 [m/s]

Similarly, for positive inclination it is seen that the average wave speed increased from the originally calculated straight tube wave form speed. Also, this waveform speed continues to increase with increasing angle of inclination. Wave form arriving time

The results obtained from these simulations are analogous to the concept of converging and diverging tube geometries discussed in Chapter 2, Section 2.4. It is seen that, there is an increase in flow velocity with an increase in the area of the channel. Likewise, there is a decrease in the flow velocity with decrease in the area of the channel.

CHAPTER 6 CONCLUSION AND FUTURE RECOMMENDATIONS

The theory behind detonation physics and pulse detonation engines was investigated. A PDE simulation having 2-D axisymmetric one-step chemical mechanism for 1-D wave propagation is modeled with a lean stoichiometric hydrogen-air mixture. It was proven that both the C-J conditions and ZND model could be successfully and accurately simulated using ANSYS FLUENT. The CJ pressure, temperature and mass fraction were calculated theoretically, obtained by the chemical equilibrium code NASA CEA. The observed C-J temperature, pressure, and velocity were all within a 10% difference, when benchmarking the solutions to NASA's CEA results.

A study was done by varying the tube dimensions to understand the influence of converging- diverging tube sections on detonation propagation and hence PDE performance. Based on the results it can be concluded that, there is an increase in flow velocity with diverging PDE tube section. Likewise, there is a decrease in the flow velocity with converging PDE tube section. However, at the time of writing this report the author was unable to find any established data to support these results.

It is known that the performance of an engine is best studied based on the thrust generated and its associated specific impulse. As present the study was concluded based on the flow velocity alone, for better conclusion it is recommended that other performance parameters also be considered while studying the effects of converging-diverging PDE tube. These other performance parameters can be obtained through multi-cycle detonations.

Bibliography

- 5 A combustion wave in a premixed gas, the Chapman-Jouguet detonation wave. (n.d.). Retrieved from https://www.mech.kth.se/courses/5C1219/Hand_out_PDF/SG2219_NT_Lecture%205%20HT10.pdf
- Anderson, J. D. (2015). *Fundamentals of Aerodynamics, Sixth Edition*. University of Maryland: McGraw-Hill Series in Aeronautical and Aerospace Engineering .
- Bonnie, J. M., & Sanford, G. (2004). CEAGui Chemical equilibrium with applications. Software Package, Ver.1.0. NASA Glenn Research Center, Cleveland, OH.
- Coleburn, N. (1964). *Chapman-Jouguet Pressures of Several Pure and Mixed Explosives*. White Oak, Maryland: US Naval Ordnance Laboratory.
- Cooper, M. a. (July 2002). The Effect of Nozzles and Extensions on Detonation Tube Performance. *AIAA Paper 2002-3628*.
- Cooper, M. J. (2002). Direct Experimental Impulse Measurements for Detonation and Deflagrations. *Journal of Propulsion and Power, Vol. 18, No. 5*, 1033-1041.
- Dupri, G., Joannon, J., R, K., & Lee, J. (1990). UNSTABLE DETONATIONS IN THE NEAR-LIMIT REGIME IN TUBES. *Twenty-Third Symposium (International) on Combustion*, 1813-1820.
- Ebrahimi, H. a. (2002). "A Numerical Simulation of a Pulse Detonation Engine with Hydrogen Fuels. *Journal of Propulsion and Power, Vol. 18, No. 5*, 1042-1048.
- Eidelman, S. G. (1991). "Review of Propulsion Applications and Numerical Simulations of The Pulse Detonation Engine Concept. *Journal of Propulsion and Power, Vol. 7, No. 6*, 857-865.
- Eidelman, S. G. (July 1990). "Air-Breathing Pulsed Detonation Engine Concept; A Numerical Study. *AIAA Paper 1990-2420*.
- Endo, T., & Fujiwara, T. (2002). A Simplified Analysis on a Pulse Detonation Engine Model. *Trans. Japan Soc. Aero. Space Sci. Vol 44, No.146*, 217-222.
- FLUENT. (2017). *Computational Fluid Dynamics, Software Package, Ver.17.0, ANSYS*.
- Garg, A., & Dhiman, A. (October, 2014). Innovative Trends in Pulse Detonation Engine, its Challenges and Suggested Solutions. *Journal of Basic and Applied Engineering Research, Volume 1, Number 4*, pp.6-10.
- Glassman, I., & Yetter, R. A. (2008). *Combustion, Fourth Edition*. Elsevier Inc. .
- Gopalakrishnan, N. (2017). *Numerical Simulation of Flow in Fluid Valves in Rotating Detonation Engines*. The University of Texas at Arlington.
- He, X. &. (2003). Numerical simulation of pulse detonation engine phenomena. *J. Sci. Comput*, 19(1-3).
- Helman, D. S. (June 1986). Detonation Pulse Engine. *AIAA Paper 1986-1683*.

- Hinke, J. B. (July 1995). Shock Tube Experiments for the Development of a Hydrogen-Fueled Pulse Detonation Engine. *AIAA Paper 1995-2578*.
- Kailasanath, K. (2009-631). Research on pulse detonation combustion systems -a status report. *AIAA J.*, 2009, doi: 10.2514/6.2009-631.
- Kailasanath, K. (n.d.). *A review of research on pulse detonation engines. Report*. Naval research laboratory.
- Korovin, L. L. (1981). Combustion of Natural Gas in a Commercial Detonation Reactor. *Fizika Gor. Vzryva*, Vol. 17, No. 3, 86.
- Krzycki, L. (1962). *Performance Characteristics of an Intermittent-Detonation Device*. U.S. Naval Ordnance Test Station, China Lake, CA: NAVWEPS Report 7655.
- Lam, M., Tillie, D., T., L., & B., M. (2004). *Pulse Detonation Engine Technology: An Overview*. The University of British Columbia.
- Lee, J. H. (2008). *The Detonation Phenomenon*. McGill University: Cambridge University Press.
- Lim, W. H. (2010-12). *Gasdynamic Inlet Isolation in Rotating Detonation Engine*. Monterey, CA: Naval Postgraduate School.
- Ma, F. (2003). *Thrust Chamber Dynamics and Propulsive Performance of Airbreathing Pulse Detonation Engines*. Pennsylvania: The Pennsylvania State University.
- Majithia, A. (2011). *Investigating the Fundamentals of Liquid- Fuelled Pulse Detonation Engines*. Cardiff University: ProQuest LLC.
- Nichollas, J. W. (1957). intermittent Detonation as a Thrust -Producing Mechanism. *Jet Propulsion*, Vol.27, No.5, 534-541.
- Rouf, H. (2003). *Parametric Study for Performance Optimization of Pulse Detonation Engines*. Bozeman, Montana: Montana State University.
- Shchelkin, K. (1940). *Soviet Journal of Technical Physics*, Vol. 10, 823-827.
- Sinibaldi, J. B. (July 2001). Ignition Effects on Deflagration-toDetonation Transition Distance in Gaseous Mixtures. *AIAA Paper 2000-3466*.
- Srihari, P., & Mallesh, M. A. (2015). Numerical Study of Pulse Detonation Engine with One-step Overall Reaction Model. *Defence Science Journal*, 265-271.
- T., B., & G., P. (1995). *Pulse Detonation Engine Theory and Concepts*. The American Institute of Aeronautics and Astronautics, Inc.
- Thattai, A. (2010). *A Validation Study for Turbulent Premixed Flame Propagation in Closed Vessels*. Delft University of Technology.
- Valli, D. M., & Jindal, T. (April 2014). Pulse Detonation Engine: Parameters. *International Journal of Innovative Research in Science*, Vol. 3, Issue 4,, 11229- 11237.

Vizcaino, J. (2013). *Investigation of Pulse Detonation Engines; Theory, Design and Analysis*. Daytona, Beach, FL: Embry-Riddle Aeronautical University, Scholarly Commons.

Watanabe, K. &. (2006-556). Numerical simulation of pulse detonation engine with a thermally perfect overall reaction model. *AIAA Paper, 2006*, doi: 10.2514/6.2006-556.

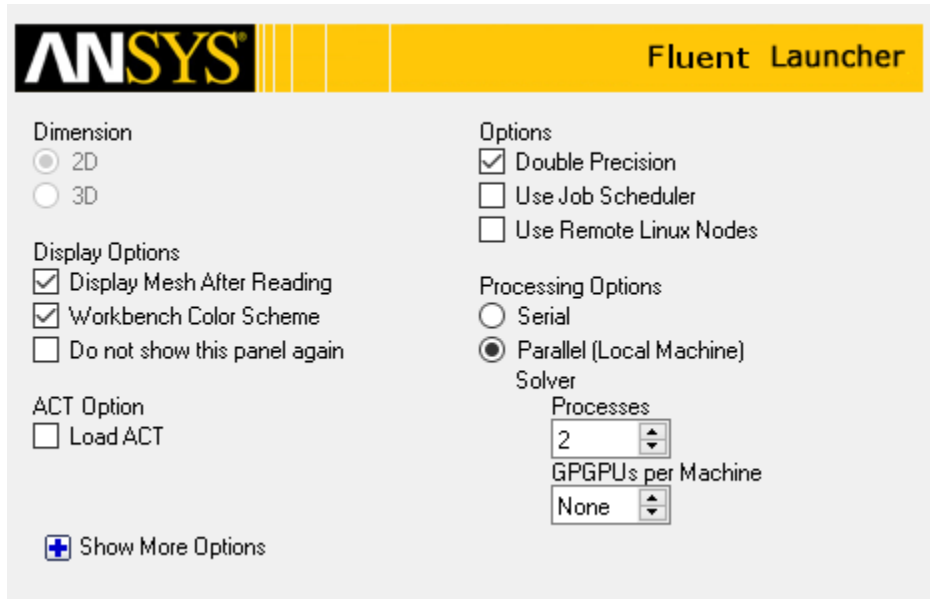
Wu, Y., & Lee, J. H. (April 2015). Stability of spinning detonation waves. *Combustion and Flame*.

Yungster, S. (2003). Analysis of Nozzle Effects on Pulse Detonation Engine Performance. *41st Aerospace Sciences Meeting and Exhibit*. Reno, Nevada: The American Institute of Aeronautics and Astronautics, Inc.

APPENDIX

Appendix A

1. FLUENT launcher setup



The image shows the ANSYS Fluent Launcher dialog box. The title bar includes the ANSYS logo and the text "Fluent Launcher". The dialog is divided into several sections:

- Dimension:** Radio buttons for 2D (selected) and 3D.
- Display Options:** Checkboxes for "Display Mesh After Reading" (checked), "Workbench Color Scheme" (checked), and "Do not show this panel again" (unchecked).
- ACT Option:** Checkbox for "Load ACT" (unchecked).
- Options:** Checkboxes for "Double Precision" (checked), "Use Job Scheduler" (unchecked), and "Use Remote Linux Nodes" (unchecked).
- Processing Options:** Radio buttons for "Serial" (unchecked) and "Parallel (Local Machine)" (selected).
- Solver:** A dropdown menu for "Processes" set to "2" and another dropdown menu for "GPGPUs per Machine" set to "None".
- Show More Options:** A button with a plus sign and the text "Show More Options".

2. Solver Setup

Type	Velocity Formulation
<input type="radio"/> Pressure-Based	<input checked="" type="radio"/> Absolute
<input checked="" type="radio"/> Density-Based	<input type="radio"/> Relative
Time	2D Space
<input type="radio"/> Steady	<input type="radio"/> Planar
<input checked="" type="radio"/> Transient	<input checked="" type="radio"/> Axisymmetric
	<input type="radio"/> Axisymmetric Swirl

3. Solution Method Setup

Formulation
Implicit
Flux Type
Roe-FDS
Spatial Discretization
Gradient
Least Squares Cell Based
Flow
Second Order Upwind
Transient Formulation
Second Order Implicit
<input type="checkbox"/> Non-Iterative Time Advancement
<input type="checkbox"/> Frozen Flux Formulation
<input type="checkbox"/> Warped-Face Gradient Correction
<input type="checkbox"/> High Order Term Relaxation
<input type="checkbox"/> Convergence Acceleration For Stretched Meshes
Options...
Default

4. Pressure Outlet Boundary Conditions

Zone Name

outlet

Momentum Thermal Radiation Species DPM Multiphase Potential UDS

Backflow Reference Frame	Absolute	
Gauge Pressure (pascal)	10	constant
Pressure Profile Multiplier	1	P
Backflow Direction Specification Method	Normal to Boundary	
Backflow Pressure Specification	Total Pressure	
<input type="checkbox"/> Average Pressure Specification		
<input type="checkbox"/> Target Mass Flow Rate		
Acoustic Wave Model		
<input checked="" type="radio"/> Off		
<input type="radio"/> Non Reflecting		

Appendix B

NASA CEA output file

UNBURNED GAS

P1, BAR	1.0132
T1, K	300.00
H1, KJ/KG	-1.65
M1, (1/n)	20.970
GAMMA1	1.4014
SON VELL, M/SEC	408.3

BURNED GAS

P, BAR	15.712
T, K	2946.93
RHO, KG/CU M	1.5368 0
H, KJ/KG	1339.35
U, KJ/KG	316.97
G, KJ/KG	-29919.2
S, KJ/(KG) (K)	10.6072
M, (1/n)	23.966
(dLV/dLP) t	-1.00966
(dLV/dLT) p	1.2086
Cp, KJ/(KG) (K)	3.3761
GAMMA s	1.1634
SON VEL, M/SEC	1090.6

DETONATION PARAMETERS

P/P1	15.507
T/T1	9.823
M/M1	1.1429
RHO/RHO1	1.8041
DET MACH NUMBER	4.8192

DET VEL, M/SEC	1967.6
----------------	--------

MOLE FRACTIONS

*Ar	0.00753
*CO	0.00011
*CO2	0.00014
*H	0.00610
HO2	0.00001
*H2	0.03254
H2O	0.29395
*NO	0.00738
*N2	0.62395
*O	0.00202
*OH	0.01903
*O2	0.00723